2015

Nanomechanical and Morphological Characterization of Tungsten Trioxide (WO3) Thin Films Grown by Atomic Layer Deposition

M. A. Mamun
Old Dominion University

K. Zhang
Old Dominion University

H. Baumgart
Old Dominion University

A. A. Elmustafa
Old Dominion University

Original Publication Citation

Mamun, M. A., Zhang, K., Baumgart, H., & Elmustafa, A. A. (2015). Nanomechanical and morphological characterization of tungsten trioxide WO_3 thin films grown by atomic layer deposition. *ECS Journal of Solid State Science and Technology, 4*(9), P398-P401. doi:10.1149/2.0241509jss

Nanomechanical and Morphological Characterization of Tungsten Trioxide (WO_3) Thin Films Grown by Atomic Layer Deposition

M. A. Mamun,[a,b] K. Zhang,[b,c] H. Baumgart,[b,c,*] and A. A. Elmustafa[a,b,z]

[a]Department of Mechanical and Aerospace Engineering, Old Dominion University, Norfolk, Virginia 23529, USA
[b]Applied Research Center, Thomas Jefferson Lab, Newport News, Virginia 23606, USA
[c]Department of Electrical and Computer Engineering, Old Dominion University, Norfolk, Virginia 23529, USA

This study investigates the nanomechanical properties and surface morphology of tungsten oxide (WO_3) thin films deposited on p-type Si (100) substrates using atomic layer deposition (ALD) technology with 2000 ALD deposition cycles at a growth temperature of 300°C and annealed at different temperatures. The samples were further furnace annealed at 500, 600 and 700°C for 60 min. The influence of the deposition process on the structure and properties of the WO_3 films is discussed, presented and correlated to the characteristic features of the ALD technique. The results depict significant difference in the hardness and modulus measurements between the as deposited sample and the annealed ones. The hardness and modulus drop from 14 and 170 GPa for the as deposited sample to 10 and 140 GPa for the annealed ones respectively. Surface roughness was observed to increase with annealing temperature and the initially amorphous as deposited sample reached complete recrystallization and transformed into polycrystalline films as indicated by XRD.
 [DOI: 10.1149/2.0241509jss]

Manuscript submitted January 12, 2015; revised manuscript received August 24, 2015. Published September 5, 2015. This was Paper 1623 presented at the Cancun, Mexico, Meeting of the Society, October 5–9, 2014.

In the past the transition metal oxide tungsten trioxide (WO_3) occurred primarily as an intermediate compound during the recovery of tungsten metal from mining ores. Today tungsten trioxide is specifically synthesized as thin films for various technological applications. Tungsten trioxide (WO_3) films possess interesting properties, making them useful in various thin-film applications, such as smart windows or flat-panel displays,[1,2] in electrochromic devices,[3] gas sensors,[3] and photo catalysis/photoconductivity.[4] Many studies have shown that tungsten oxide experiences elecrochromic color changes.[5–9] It is postulated that electro-coloration of tungsten oxide is the result of a double injection of cations and electrons into the host lattice.[10] Theoretical calculations and experimental observations confirmed polymorphism of tungsten oxide crystals.[11–25] Tungsten trioxide has been utilized for a long time for the manufacture of X-ray screen phosphors. In recent years tungsten trioxide has been successfully employed in the industrial fabrication of electrochromic windows. These smart windows receive a thin coating of tungsten trioxide with transparent electrical contacts that allow changing the light transmission properties through the window with an applied voltage. Such a WO_3 coating on the window glass enables modulation of the amount of tint of the window as a function of the applied voltage, changing the amount of light or heat passing through. The newest generation of modern aircraft has already implemented such actively switched smart windows with high technology thin film coatings. Tungsten oxides are also known for their use as solid lubricants at elevated temperatures and they have been used as powdery materials for tribological coatings or as component of ceramics.[26] In addition WO_3 is one of the more popular compounds for water splitting research with an extensive body of literature. However, only recently has ALD been successfully utilized to synthesize tungsten oxide WO_3 films as catalyst for water splitting into hydrogen and oxygen.[27] Many of these applications especially as solid lubricants at elevated temperatures, powdery materials for tribological coatings, components of ceramics, and electrochromic devices are strongly dependent on tungsten oxide's crystal morphology, microstructure, and mechanical properties. The fabrication techniques and conditions strongly influence the microstructure, which in turn impacts the electrochromic behavior and degradation of the films.[28] Also the mechanical properties are closely related to the microstructure and can affect the durability and stability of the electrochromic devices associated with any mechanical damage.[29] Tungsten trioxide is monoclinic at room temperature and moderate temperatures until 330°C. If heated at temperatures above 740°C, tungsten trioxide is tetragonal. At intermediate temperatures in the range of 330°C until 740°C WO_3 films exhibit orthorhombic crystal structure. Aside from tungsten trioxide WO_3 or Tungsten (VI) oxide there exist other tungsten oxides, notably WO_2, which is highly electrically conductive and which is obtained by reduction of WO_3.

Sample Fabrication

The ALD tungsten trioxide WO_3 films were deposited on native oxide covered (100) oriented Si substrates of four inch diameter by a thermal ALD synthesis process in a Savannah 100 cross-flow reactor from Ultratech Cambridge Nanotech. For this study tungsten hexacarbonyl $W(CO)_6$ of 99.9% purity was chosen as ALD tungsten precursor 1 and H_2O vapor from deionized DI water was used as oxidation precursor 2 source. The DI H_2O vapor of ALD precursor 2 acted as oxidizing agent to complete the reaction for the synthesis of ALD tungsten trioxide WO_3 films. Nitrogen was used as a carrier gas at a flow of 20 standard cubic centimeters per minute (sccm) and also served as the purge gas. ALD tungsten trioxide WO_3 film depositions were carried out over the reactor temperature range of 150°C to 320°C in order to establish the optimum ALD process window. The final ALD growth temperature of the WO_3 thin films was set at 300°C. The Tungsten trioxide films were deposited on a native silicon oxide covered (100) Si substrate with the following ALD growth conditions: the pulse time of the ALD precursor # 1 H_2O was 0.05 s, the purging time was 5 s, the pulse time of ALD precursor #2 $W(CO)_6$ was 0.5 s and the purging time was 5 s. The base pressure was 20 mTorr. Following successful ALD synthesis, the WO_3 films were subsequently annealed for 60 min in a quartz tube furnace at atmospheric pressure with O_2 flow at temperature range of 500 to 700°C in order to ensure optimum crystallinity and solid phase grain growth.

Experimental

Tungsten hexacarbonyl $W(CO)_6$ is a solid ALD precursor with a melting point at 170°C, which requires pre-heating of the stainless steel precursor cylinder. The vapor pressure of solid $W(CO)_6$ at 67°C is 1.2 mmHg and yielded satisfactory thin film results in our experiments when reacted with DI H_2O. In contrast to our work the only previous ALD studies on the synthesis of WO_3 films utilized a different metal organic precursor bis(tert-butylimido)bis(dimethylamido)-tungsten(VI) $(tBuN)_2(Me_2N)_2W$.[27] In our investigation ALD synthesis with tungsten hexacarbonyl $W(CO)_6$ and deionized H_2O resulted in

*Electrochemical Society Active Member.
zE-mail: aelmusta@odu.edu

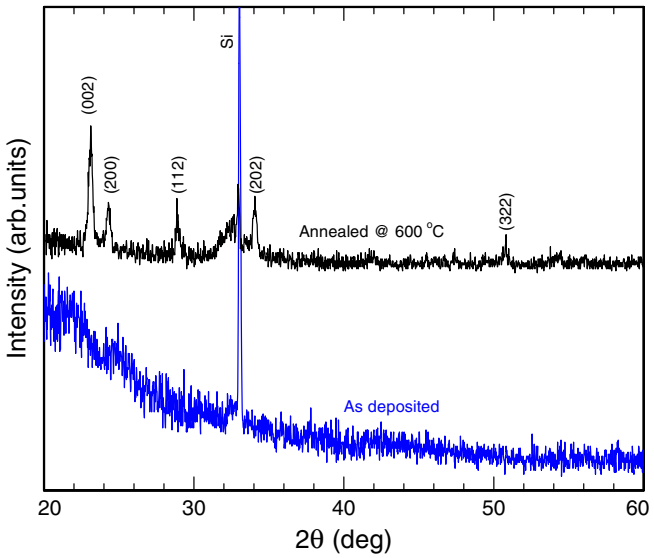

Figure 1. X-ray diffraction of ALD WO_3 thin films shows an amorphous phase of as-deposited ALD films at 300°C for ALD 2000 cycles on Si substrates and a polycrystalline WO_3 structure after post-deposition annealing at 600°C for 60 min.

good crystalline WO_3 films following subsequent furnace annealing. The surface morphology and roughness parameters of the ALD deposited WO_3 films were determined by AFM measurements. For this study we focused on conducting nanoindentation testing to investigate the mechanical properties of the ALD WO_3 thin films. A nanoindenter XP equipped with a three sided Berkovich diamond tip was used in conjunction with the continuous stiffness method in depth control mode to measure the hardness and modulus of the WO_3 thin films. The CSM method enables the continuous evaluation of the mechanical properties of materials as a function of the contact depth as detailed elsewhere.[30] As our standard experimental procedure a total of 15 indents with maximum indentation depth of 500 nm were performed on each sample. The allowable drift rate and the strain rate for loading were specified as 0.05 nm/s and 0.05 s^{-1} respectively. During the loading of the indenter the WO_3 thin film material undergoes elastic and plastic deformation.

Results and Discussion

The X-ray diffraction (XRD) analysis of Figure 1 indicates that the as deposited ALD WO_3 thin film at 300°C was initially amorphous. The ALD films of Figure 1 recrystallized and transformed into polycrystalline films subsequent to thermal annealing at 600°C for 60 min under atmospheric condtions.

The AFM micrographs of Figure 2 highlight the surface morphology of films grown with 2000 ALD deposition cycles for as the deposited sample and annealed samples with a temperature range from 500 to 700°C. The 3-D AFM micrograph of Figure 2a displays an as deposited sample with a relative smooth surface interspersed with some larger grains, while Figure 2b represents a the film annealed at 500°C, whereas Figures 1c and 1d represent a 3 D AFM micrograph of the films annealed at 600 and 700°C respectively. Higher annealing temperature results in increased surface roughness The root mean square roughness of the film surfaces were analyzed as 1.03, 1.12, 1.26, and 1.6 nm respectively for the as deposited and the 500, 600, and 700°C annealed samples. This indicates that the rms surface roughness increases as a function of the post-deposition furnace annealing temperature The analysis of the AFM images of Figure 2 revealed a steady decrease in the grain with thermal annealing. The grain height was measured as 10.9, 9.7, 8.3, and 6.3 nm for the as deposited and the 500, 600, and 700°C annealed samples. The grain

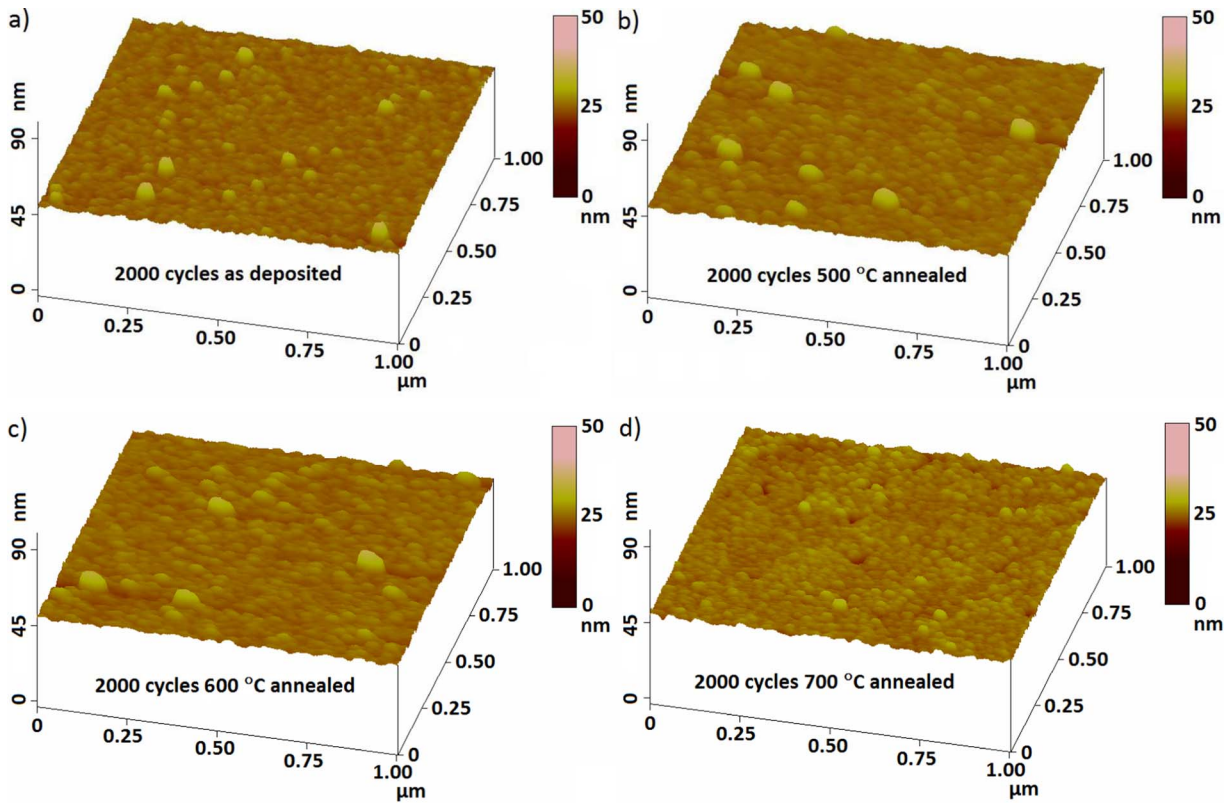

Figure 2. AFM micrographs of the surface morphology of 2000 ALD cycles WO_3 samples (a) As deposited, (b) 500°C thermally annealed (c) 600°C thermally annealed (d) 700°C thermally annealed.

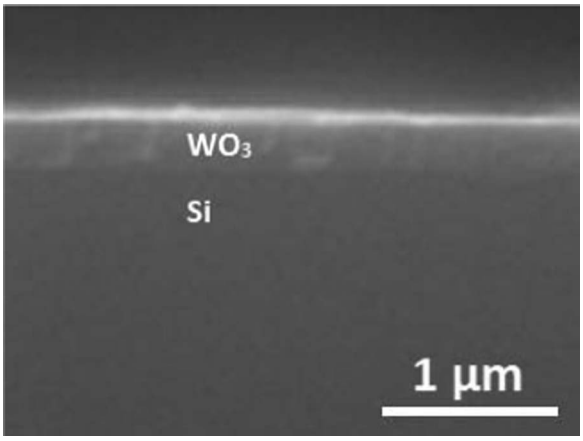

Figure 3. FE-SEM micrographs of surface morphology cross-section of as-deposited WO_3 films grown at 300°C with 2000 ALD cycles on Si substrates.

size of the as deposited sample was 51 nm and 58.9, 58.8, and 39.2 nm for the 500, 600, and 700°C annealed samples respectively.

The as-deposited WO_3 thin films surface morphology was characterized by FE-SEM as shown in Figure 3. It is clearly evident from the surface of the as-deposited films with 2000 ALD cycles at 300°C growth temperature that the deposition was uniform and the film is approximately 40 nm thick. The resulting growth rate in these films saturated to around 0.2 Å/ALD cycle.

Among the nanomechanical properties of interest in this study of these ALD WO_3 films are the hardness and the modulus. The nanoindentation hardness is defined as the indention load divided by the projected contact area of the indenter tip and the modulus is calculated from the contact stiffness and the contact area. The hardness and modulus results versus contact depth of indentation are shown in Figures 4 and 5. The scatter in the nanomechanical measurements from different indents on each sample is illustrated as 3σ error bar, where σ is the standard deviation. The hardness plotted as a function of indentation depth in Figure 4 shows that the crystalline WO_3 ALD films annealed at 500, 600, and 700°C have a hardness of approximately 13 GPa, which is harder than the single crystal Si substrate of 12 GPa. As the indenter proceeds deeper into the film and eventually reaches into the Si substrate underneath, the hardness value

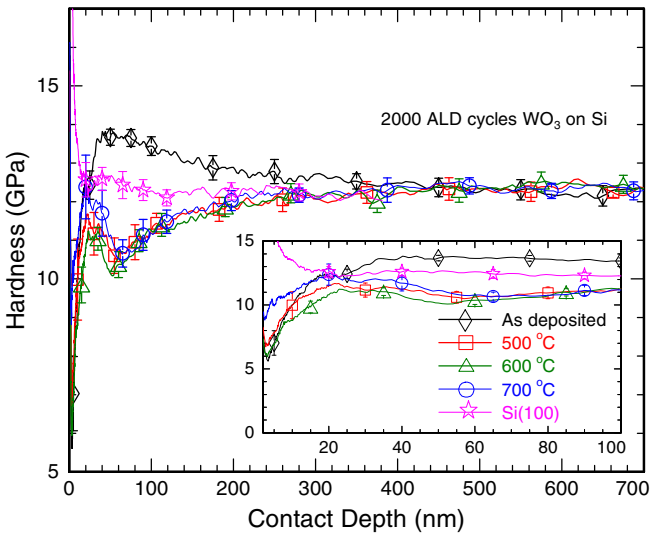

Figure 4. Hardness versus contact depth of indentation for as deposited, and 500, 600, and 700°C thermally annealed WO_3 films grown at 300°C with 2000 ALD cycles.

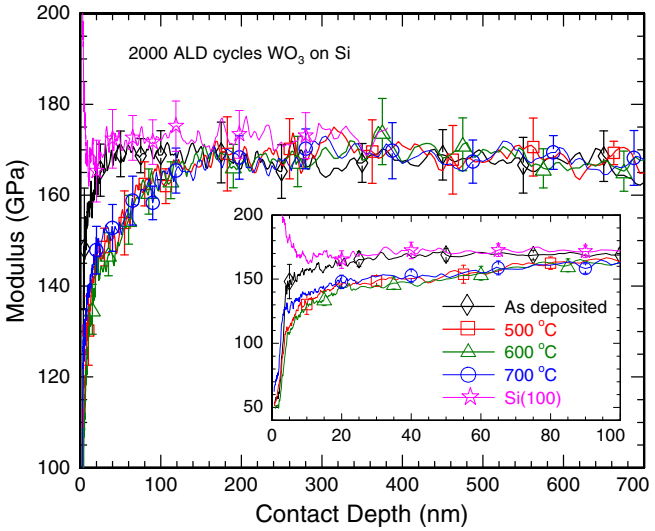

Figure 5. Modulus versus contact depth of indentation for as deposited, and 500, 600, and 700°C thermally annealed WO_3 films grown at 300°C with 2000 ALD cycles.

converges to the expected bulk Si value of 12 GPa. The plot of Figure 4 reveals that the hardness drops subsequent to thermal annealing of the as deposited samples, which indicates a softening of the ALD WO_3 film when thermally annealed. Similar trends were also observed for the modulus measurements as depicted by the plot of Figure 5. The results depict significant difference in the hardness and modulus measurements between the as deposited sample and the annealed ones. The hardness and modulus drop from 14 and 170 GPa for the as deposited sample to 10 and 140 GPa for the annealed ones respectively.

Conclusions

In summary, the nanoindentation hardness of WO_3 ALD synthesized films has been determined as 14 GPa and the modulus was found to be 170 GPa for the as deposited samples. As the samples are subsequently thermally annealed, the indentation hardness is observed to decrease. The modulus also drops from 170 GPa of the as deposited samples to 140 GPa when the samples were thermally annealed.

Acknowledgment

The authors acknowledge the college of William and Mary's materials characterization lab for the AFM microscopy images.

References

1. C.-G. Granqvist, *Handbook of Inorganic Electrochromic Materials*, Elsevier, Amsterdam (1995).
2. P. Tägtström, P. Mårtensson, U. Jansson, and J.-O. Carlsson, *J. Eectrochem. Soc.*, **146**, 3139 (1999).
3. K. Bange, *Sol. Energy Mater. Sol. Cells*, **58**, 1 (1999).
4. M. Boulova, A. Gaskov, and G. Lacazeau, *Sens. Actuators, B, Chem.*, **81**, 99 (2001).
5. R. S. Crandall and B. W. Faughnan, *Appl. Phys. Lett.*, **26**, 120 (1975).
6. B. Reichman and A. J. Bard, *J. Electroehem. Soc.*, **126**, 583 (1979).
7. T. Kamimori, J. Nagai, and M. Mizuhashi, in *Proc. SPIE*, **428**, 51 (1983).
8. H. Tada, in *Large-Area Chromogenics: Materials and Devices for Transmittance Control*, C. M. Lampert and C. G. Granqvist, Editors, SPIE Institute Series **IS.4**, 230 (1990).
9. S. K. Deb, in *Proc. Symp. on Electrochromic Materials*, M. K. Carpenter and D. A. Corrigan, Editors, **90–2**, 3 (1990).
10. O. Bohnke, M. Rezrazi, B. Vuillemin, C. Bohnke, P. A. Gillet, and C. Rousselot, *Sol. Energy Mater. Sol. Cells*, **25**, 361 (1992).
11. S. Tanisaki, *J. Phys. Soc. Jpn.*, **15**, 566 (1960).
12. B. O. Loopstra and P. Boldrini, *Acta Crystallogr. B*, **21**, 158 (1966).
13. B. O. Loopstra and H. M. Rietveld, *Acta Crystallogr. B*, **25**, 1420 (1969).
14. E. Salje and K. Viswanathan, *Acta Crystallogr. A*, **31**, 356 (1975).
15. E. Salje, *Acta Crystallogr. A*, **31**, 360 (1975).

16. E. Salje, *Acta Crystallogr. B*, **33**, 574 (1977).
17. R. Diehl, G. Brandt, and E. Salje, *Acta Crystallogr. B*, **34**, 1105 (1978).
18. T. Hirose, *J. Phys. Soc. Jpn.*, **49**, 562 (1980).
19. P. W. Woodward, A. W. Sleight, and T. Vogt, *J. Phys. Chem. Solids*, **56**, 1305 (1995).
20. K. L. Kehl, R. G. Hay, and D. Wahl, *J. Appl. Phys.*, **23**, 212 (1952).
21. E. K. H. Salje, S. Rehmann, F. Pobell, D. Morris, K. S. Knight, T. Herrmannsdörfer, and M. T. Dove, *J. Phys. C: Condens. Matter*, **9**, 6563 (1997);E. Salje, *Ferroelectrics*, **12**, 215 (1976).
22. E. Iguchi, H. Sugimoto, A. Tamenori, and H. Miyagi, *J. Solid State Chem.*, **91**, 286 (1991).
23. I. Lefkowitz, M. B. Dowell, and M. A. Shields, *J. Solid State Chem.*, **15**, 24 (1975).
24. J. B. Goodenough, *Prog. Solid State Chem.*, **5**, 145 (1971).
25. F. B. Li, G. B. Gu, X. J. Li, and H. F. Wan, *Acta Phys. Chim. Sin.*, **16**, 997 (2000).
26. E. Lugscheider, S. Bärwulf, and C. Barimani, *Surf. Coat. Technol.*, **102–121**, 458 (1999).
27. Rui Liu, Yongjing Lin, Lien-Yang Chou, Stafford W. Sheehan, Wangshu He, Fan Zhang, Harvey J. M. Hou, and Dunwei Wang, *Angew. Chem. Int. Ed.*, **50**, 499 (2011).
28. C. G. Granqvist, *Handbook of Inorganic Electrochromic Materials*, Elsevier, Amsterdam, The Netherlands, 1995, p. 33.
29. C. W. Ong, H. Y. Wong, G. K. H. Pang, K. Z. Baba-Kishi, and C. L. Choy, *J. Mater. Res.*, **16**, 1541 (2001).
30. W. C. Oliver and G. M. Pharr, *J. Mater. Res.*, **19**, 3 (2004).